

Dedicated to Prof. Dorin N. Poenaru's  
70th Anniversary

## ISLAND OF THE HIGH YIELDS OF $^{252}\text{Cf}(\text{sf})$ COLLINEAR TRIPARTITION IN THE FRAGMENT MASS SPACE

Yu.V. PYATKOV<sup>1,2</sup>, D.V. KAMANIN<sup>1</sup>, W.H. TRZASKA<sup>3</sup>,  
W. VON OERTZEN<sup>4</sup>, S.R. YAMALETDINOV<sup>3</sup>, A.N. TJUKAVKIN<sup>1</sup>,  
V.G. TISHCHENKO<sup>1</sup>, **V.G. LYAPIN<sup>3</sup>**, YU.E. PEINIONZHKEVICH<sup>1</sup>,  
A.A. ALEXANDROV<sup>1</sup>, S.V. KHLEBNIKOV<sup>5</sup>

<sup>1</sup>Joint Institute for Nuclear Research, Flerov Laboratory of Nuclear Reactions  
141980 Dubna, Moscow Region, Russia, E-mail: kamanin@fobos.jinr.ru

<sup>2</sup>Moscow Engineering Physics Institute

115409 Moscow, Russia, E-mail: yvp\_nov@mail.ru

<sup>3</sup>Department of Physics of University of Jyväskylä, Finland

<sup>4</sup>Hahn-Meitner-Institute GmbH Str. 100, 14109 Berlin, Germany

<sup>5</sup>Khlopin- Radium – Institute, 194021, St. Petersburg, Russia

(Received January 23, 2007)

*Abstract.* Results of three independent experiments aimed at searching for collinear cluster tripartition (CCT) of the  $^{252}\text{Cf}(\text{sf})$  are reported. They confirm previously proposed kinematical scheme let to distinguish two CCT partners flying almost in the same direction. A new island of the CCT manifestation in the mass-mass distribution of the decay fragments was revealed. A total yield of the CCT originated events in the island is not less  $4 \cdot 10^{-3}$  per binary fission. Presumably, the ternary decay of nuclear molecules based on heavy magic clusters such as isotopes of Ni, Ge, Sn, Te gives rise to the effect observed.

*Key words:* clustering, multibody decays, shell effects, fission.

### 1. INTRODUCTION

Fission of low excited heavy nuclei into three fragments of comparable masses, the so-called “true ternary fission” has not been reported so far despite multiple attempts to find such a decay channel till yearly fifties of last century [1]. Fragmentation of the cold nuclear matter is of grate interest in

view of a nuclear quantum, structural effects that stand behind. One of the brightest among them is the heavy ion or cluster radioactivity when a strongly bounded nucleus close to Pb, being double magic, is preformed and emitted in the body of the mother system. Often this type of decay is called “lead radioactivity”. This extremely rare phenomenon is observed with a probability  $10^{-10} - 10^{-17}$  relative to usual  $\alpha$ -decays [2]. In our previous publications [3, 4, 5], we have reported a new spontaneous ternary decay channel in  $^{252}\text{Cf}$  being much more probable due to a link with magic constituents. It was called “collinear cluster tri-partition” (CCT) because the decay products fly apart almost collinearly. In order to distinguish the CCT event from the binary fission one, we used different gating such as selection by neutron multiplicity [6], velocity, momentum, and their combinations. Due to this procedure, we succeeded to reveal some different ternary decay modes that manifested themselves via pronounced structures in the mass-mass distributions of the detected fragments. The yield of each mode amounted to approximately  $10^{-5}$  per binary fission. Here we report a series of experiments that let us find a new island of high CCT yields in the mass-mass distribution of the fragments originated from  $^{252}\text{Cf}$  (sf).

## 2. EXPERIMENTAL PROCEDURE

In the present work, we describe the results of three experiments devoted to the search for collinear tripartition of the  $^{252}\text{Cf}$  nucleus. Among all known methods of measuring the masses of nuclear reaction products, the TOF-E (time-of-flight versus energy) method is the only one which uniquely allows the study of multibody decays. In this method both, the fragment velocities  $V$ , obtained by means of TOF, and the energy  $E$  are measured for each fragment individually. The fragment mass  $M$  is calculated simply using  $M = 2E/V^2$ . Three different TOF-E spectrometers with the detector arms placed opposite to each other and symmetric to the  $^{252}\text{Cf}$  source were used in our experiments as described below.

In the first experiment (Ex1, Fig. 1a), performed at the FOBOS setup at the Flerov Laboratory (FLNR) of the Joint Institute for Nuclear Research in Dubna [7], about  $13 \cdot 10^6$  coincident binary fission events were recorded (the numbers in parenthesis refer to labels in the figure). The TOF of the fragments was measured over a flight path of 50 cm between the start detector(3) based on the micro-channel plates (MCP) placed next to the  $^{252}\text{Cf}$  source(1) and the stop position-sensitive avalanche counters (PSAC,4). The latter provided through the measurements of the position also the fragment emission angle with a precision of  $0.2^\circ$ . The energies of the coincident fragments that passed

through the PSACs were measured in the Bragg ionization chambers (BIC, 5) with entrance windows supported by a grid (6) with 70 hexagonal, the side view is shown in the insert (left) of Fig. 1.

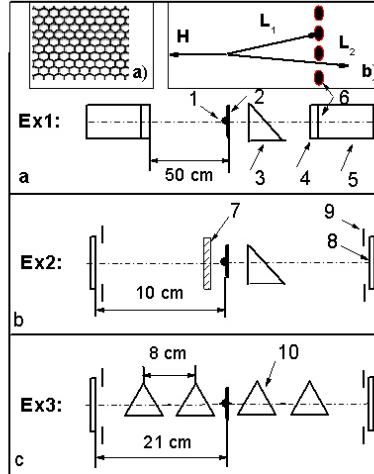


Fig. 1 – A scheme of coincident measurements of two fragments of the collinear tripartition partners for the three experiments. The first experiment, Ex1(a) was performed at the FOBOS setup. Here: 1 is a Cf source; 2 is a source backing; 3 is a microchannel plate (MCP) based timing start detector; 4 is a position-sensitive avalanche counter as stop detector; 5 is an ionization chamber with the supporting grid(6) on the entrance window. The side view of the grid is shown in the insert (left). The second and third experiments, Ex2, Ex3 (b and c) were performed at the spectrometers based on MCP detectors(2,10) and PIN diodes(8) bounded by a frame(9). The scheme of detecting of the tripartition partners is shown in the insert (right). After passage of the dispersion foil, two light fragments(L1 and L2) obtain a small-angle divergence due to multiple scattering. One of the fragments(L1) can be lost hitting the separating block, while the fragment L2 reaches the energy detector.

This mechanical structure of the detectors is essential for the registration of the effect described below (see Section 2). The  $^{252}\text{Cf}$  source is mounted on  $\text{Al}_2\text{O}_3$  backing(2) of a thickness  $50 \mu\text{g}/\text{cm}^2$ , the other side was free or coated with a layer of Au of  $20 \mu\text{g}/\text{cm}^2$  thickness. In Fig. 1, insert (right), the primary heavy fragment(H) is emitted to the left from the free side of the  $^{252}\text{Cf}$ -source; the two light fragments (L1 and L2) are emitted in the same direction. As explained below, scattering processes will separate the two light fragments in a small angular separation, and only one of them is likely to be registered. If both fragments enter, only the total energy is measured. A similar source of

$^{252}\text{Cf}$  was used in further experiments performed at the Accelerator Laboratory of the University of Jyväskylä (JYFL).

In the second experiment (Ex2, Fig. 1b) we used a different TOF-E-spectrometer based on one MCP start detector and two PIN diodes(8), the latter provided both time and energy signals. An active area of each PIN diode was bounded by the frames(9). The flight paths here were 10 cm for each detector arm. An Al foil(7), 5  $\mu\text{m}$  thick, has been placed just near active  $^{252}\text{Cf}$  layer. In this experiment,  $2 \cdot 10^6$  binary events were registered.

In the third experiment (Ex3, Fig. 1c) two pairs of the MCP-based timing detectors(10) provided signals for measuring TOFs with flight paths of 8 cm each. The fragment energy was measured by PIN diodes. The total transparency of each arm amounted to 70% due to the grids of the electrostatic mirrors (four per detector, instead of two as in the Ex1 and Ex2) of the timing detectors. In this third experiment,  $2 \cdot 10^6$  of binary events were collected.

### 3. RESULTS ON COINCIDENT FISSION EVENTS

In Fig. 2, top, we show in a logarithmic scale the two-dimensional (2D) distribution of the two registered masses of the coincident fragments in the experiment (Ex1) at the FOBOS set up. Only collinear events in both identical spectrometer arms with a relative angle of  $180 \pm 1^\circ$  were selected, this value is within the angular resolution, and it is in the range of a typical angular spread for conventional binary fission fragments. The tails in the mass distributions marked 3-6 in Fig. 2, top, extending from the loci(1 and 2) used to mark the conventional binary fission, are mainly due to the scattering of the fragments on both the foils and on the grid edges of the stop avalanche counters and the ionization chambers. An astonishing difference in the shapes of the tails(3 and 4) attracts attention. The only small but important asymmetry between the two arms to be emphasized consists in a very thin source backing for the rear side and the start detector foil located in the arm b only (Fig. 1, top). There is a distinct bump, marked(7), on the latter tail(4), oriented approximately parallel to the line defining a constant sum of masses,  $M_a + M_b = \text{const.}$ , i.e., tilted by  $45^\circ$  with respect to the abscissa axis. The explanation of this bump is the essence of our analysis. The bump is located in a region corresponding to a large missing mass. In Fig. 2, top, we show the line for the total mass  $M_{total} = 225$  as a border line to separate these interesting events from normal binary fission. A statistical significance of the events in the structure(7) can be deduced from Fig. 2, bottom. There the spectra of total masses,  $M_{total} = M_a + M_b$ , for the tails(4 and 3), spectrum *a* and spectrum *b*, respectively,

are compared. The difference spectrum of  $b$  and the tail(3) is marked  $c$ , the integral of these events is  $4.7 \cdot 10^{-3}$  relative to the conventional fission events contained in the locus(2), shown in Fig. 2, top. The corresponding ratio for the gross peak of the curve  $a$  (shown by the dashed line) is smaller and amounts to about  $2.7 \cdot 10^{-3}$ . A background as shown was defined by a polynomial fit (curve  $d$ ) using the points outside the peak.

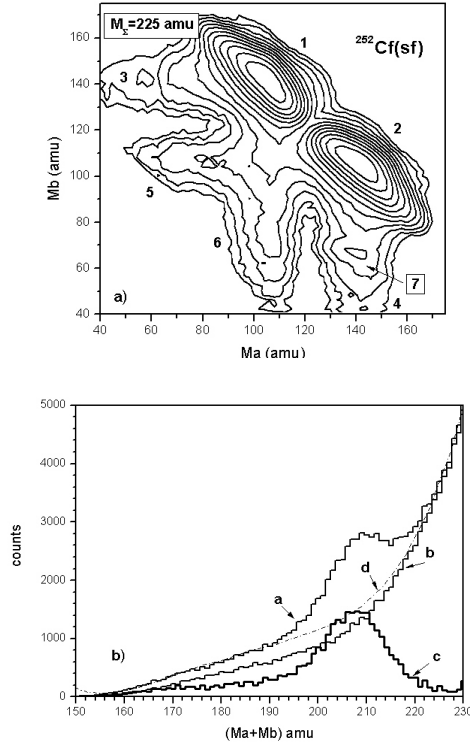


Fig. 2 – Experimental evidence of the collinear tripartition of  $^{252}\text{Cf}$  obtained at the FOBOS setup. Contour map (in logarithmic scale) of the mass-mass distribution of the collinear fragments detected in coincidence in the opposite arms (marked by letters  $a$  and  $b$ ) of the spectrometer (top). The loci of conventional binary fission events 1, 2 are prolonged by the tails marked 3-6 due to the scattered fragments. Bump 7 located below the line of the sum  $M_a + M_b = 225 \text{ a.m.u.}$  is analyzed (bottom). There the spectra of total masses for the tails(3 and 4), spectrum  $a$  and spectrum  $b$ , respectively, are compared. The difference spectrum is marked  $c$ . Curve  $d$  is a polynomial fit using the points outside of the gross peak on spectrum  $a$ .

In order to explain the differences in the tails(3 and 4) mentioned above, the following scenario is proposed, the geometry is shown in Fig. 1, insert (right). In ternary fission, the three fragments are emitted collinearly and two

of the fragments are emitted in one direction but become separated with an angle less than  $1^\circ$  after passing a dispersing media, due to multiple scattering [8]. These materials are the backing of the source (located only on the side of tail(4) or the Al foil placed deliberately in the path). If both fragments pass on and enter into the (BIC), we register a signal corresponding to the sum of the energies of the two fragments. The event is registered as binary fission with almost usual parameters. In the other scenario, only a proper energy (mass) of one of the light fragments is measured, because the second one is stopped (lost) in the supporting grid of the ionization chamber or for the other cases in the frame of the PIN diode playing the role of a separating element.

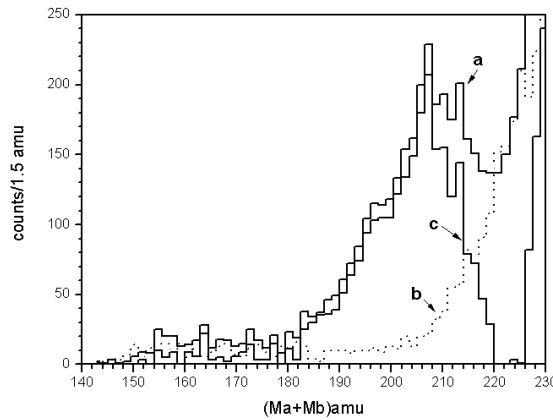


Fig. 3 – Spectrum of sum of masses ( $M_a + M_b$ ) from experiment Ex2, for two registered fragments for the gate similar to the tail 4 from Fig. 2, top, spectrum *b* corresponds to the clean opposite arm free from dispersion foil, *c* is the difference spectrum.

In order to verify whether the dispersive scattering through a transparent foil can give rise to the effect discussed, we have performed a special experiment (Ex2, Fig. 1b) at the JYFL spectrometer. One side of the Cf source was covered by an Al foil(7) of a  $5\mu\text{m}$  thickness. This thickness corresponds approximately to a half of the range of a typical heavy fragment. A bump similar to that shown in Fig. 1a is observed. The result of this experiment is shown in Fig. 3, which depicts the spectra analogous to those presented in Fig. 2, bottom. The bump obtained with the difference marked *c*, again appears in the arm pointing to the scattering foil. The integrated yield of the spectrum *c* confined within the masses of 180-220 a.m.u. amounts to  $2.4 \cdot 10^{-3}$  relative to the corresponding locus of conventional binary fission. These events typically correspond to a mass loss of 40-70 a.m.u., as in the other case, the positions in the mass scale of the peaks *c* agree well in both experiments. This result also

shows that the effect of the dispersive scattering considered does not depend on the foil thickness.

In the third experiment (Ex3, Fig. 1c) the grids supporting the foils of the two MCPs used as timing detectors in each arm, served both as a separating mesh and as a dispersing media, the system has 72% total transparency within the geometrical solid angle. The energy was obtained by PIN diodes. Again the separation of the two lighter partners of the tripartition decay was achieved by scattering in a dispersive foils and the blocking one of the two fragments (scattered at a very small relative angle) in the frames. We observe again the bump in the sum spectrum of  $M_{total} = M_a + M_b$  confined within 180-220 a.m.u. as shown in Fig. 4. Spectrum *a* corresponds to the arm facing

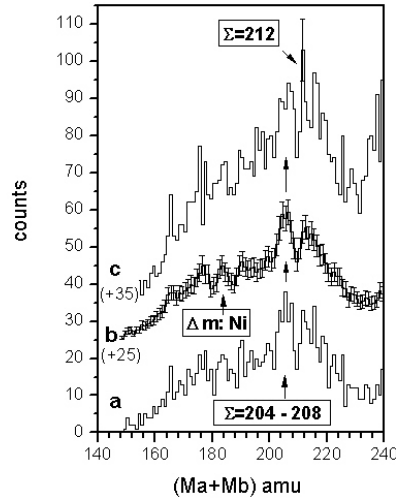


Fig. 4 – Spectrum of the sum of masses of two detected fragments obtained in our third experiment Ex3: from the arm facing the source backing (a); the same spectrum smoothed by means of averaging of counts in three adjacent channels (shifted up by 25 counts) (b); the sum of spectrum *a* and a complementary spectrum obtained in the second arm of the spectrometer (shifted up by 35 counts) (c). The sums marked in the panels correspond to different pairs of magic nuclei (see text). The peak in spectrum *b* marked by arrow is due to the doublet of missing  $^{70,68}\text{Ni}$  fragments.

the source backing, which acts as scattering medium. The additional yield mass in the same mass range as previously, relative to binary events, amounts to  $2.7 \cdot 10^{-3}$ . The best mass resolution among our experiments ( $< 2.5$  a.m.u.) was achieved in this case. This is due to the better measurement of TOFs by the MCP detectors and the absence of straggling in the energy channel. Unfortunately, the spectrum suffers from low statistics, this is partially overcome

by applying of a simple averaging procedure on the counts in three adjacent channels (curve *b*). This procedure smoothes the background fluctuations and produces two statistically reliable wide peaks in this spectrum, marked by arrows indicating missing  $^{70,68}\text{Ni}$  fragments and also by total mass of two registered fragments amounting to 204-208 a.m.u., respectively. The symmetry of the two spectrometer arms is reflected in the result that the spectrum *a* and the complementary one obtained in the second arm of the spectrometer depicted in Fig. 4 as curve *c* give the same result. The statistically significant regions centered at  $M_{total} = 204 - 212$  a.m.u. are marked by arrows in Fig.4.

We note that the same effect of an enhanced yield corresponding to a missing mass defined by a region of  $M_{total} = M_a + M_b = 180 - 212$  has been observed in the three independent experiments described. The small variation of the yields relative to the total binary events can be traced back to the different geometries. Possible uncertainties of the effect yields referred from the experiments at hand need some comments. A statistical error in any cases does not exceed 2.5%. At the same time, a systematic component is hardly to be estimate. The ratio number of ternary events per binary fission is governed via multiple scattering angles by the mass-energy-charge distribution of the ternary decay products unknown in detail. Thus we can only claim that the effect should not be less than  $4 \cdot 10^{-3}$  per binary fission.

#### 4. DISCUSSION OF THE RESULTS

The experimental observations will be interpreted as a collinear ternary decay with three fragments of a similar mass, a decay which is different than the previously reported ternary fission, where the third light fragment (typically He or Be isotopes) is emitted perpendicular to the axis spanned by the heavy fission fragments [9]. For a more detailed discussion, we come back to the results obtained in Ex1. The contour map of the two-dimensional mass-mass distribution obtained by subtraction of the tail(3) from tail(4), already defined in Fig. 1a, is shown in Fig. 5a. This distribution shows the contour of the ternary mass splits more clearly, it is almost free from further experimental background originating from scattered fragments of the normal binary fission. Some features of this 2D plot can be further emphasized by a process, where a second derivative filter is applied, a method which is typically used in the search for peaks in gamma spectra [10, 11] (Fig. 5b). The scale of the squares is defined in the insert to this figure. The tops of the peaks are found over certain linear sections of  $M_a = \text{const.}$  with intersections with the discrete diagonal lines, as marked in Fig. 5b, they correspond to the total masses  $M_{total} = \text{const.}$  with values of 204, 208 and 212 a.m.u., respectively. The listed

peaks have already been marked in Fig. 4. Thus, the bump(7) seen in Figs. 1a and 5a consists mainly of the three overlapping ridges oriented along the lines  $M_{total} = \text{const.}$

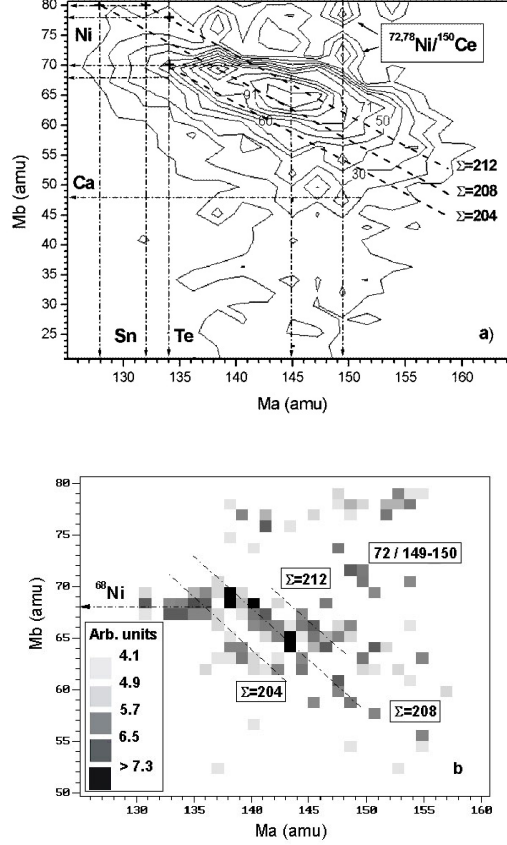


Fig. 5 – a) The figure depicts as a 2D-contour map ( $M_b$  versus  $M_a$ ) the difference between the tails(3 and 4) of the events measured with the FOBOS-detector system shown in Fig. 1a; note the expanded scale for the lighter mass fragments. Dashed lines tilted by  $45^\circ$  with respect to the  $M_a$  axis correspond to the fixed total mass of detected fragments (see the text for more details). Part *b* is the same as *a* but passed through a filter which emphasizes the two-dimensional structures.

From the observed mass spectra, we will have to consider a ternary fission process with one heavier and two lighter fragments. The missing masses in the sum spectra of the experiment (Ex1) suggest subsystems with particular masses. The same mass values are observed as distinct peaks in Fig. 4 (from Ex3); these are also seen as ridges in Fig. 5b. We note that from these data

the shell closures [12] in proton and neutron number are decisive for the formation of the emitted subsystems. As can be deduced from Fig. 5a, the ridges (marked by the dashed lines) go through crossing points corresponding to different combinations of two fragments with magic nucleon numbers (marked by the dot-and-dash arrows). These marked points could be related to mass values with magic subsystems well-known from binary fission [12, 13] as follows:  $204 \rightarrow {}^{70}\text{Ni} + {}^{134}\text{Te}$  or  ${}^{72}\text{Ni} + {}^{132}\text{Sn}$  (missing  ${}^{48}\text{Ca}$ ),  $208 \rightarrow {}^{80}\text{Ge} + {}^{128}\text{Sn}$  (missing  ${}^{44}\text{S}_{28}$ ) and for  $M_{total} = 212 \rightarrow {}^{80}\text{Ge} + {}^{132}\text{Sn}$  or  ${}^{78}\text{Ni} + {}^{134}\text{Te}$  or  ${}^{68}\text{Ni} + {}^{144}\text{Ba}$ .

It should be noted that the central peak in the Fig. 4a (marked as  $\Sigma = 204 - 208$ ) is likely a triplet which includes the peak centered at 206 a.m.u. It could be related to magic subsystem:  $206 \rightarrow {}^{72}\text{Ni} + {}^{134}\text{Te}$  (missing  ${}^{46}\text{Ar}_{28}$ ). Thus, three subsystems from these proposed above consist of three magic clusters each. The ridges discussed are crossed as well by the horizontal ridge (seen via bunching of contour lines in Fig. 1c), this effect can be linked with the isotopes of  ${}^{68,70}\text{Ni}$ , which are also magic [13]. This observation would imply that the detected light fragment from the two  $L_1, L_2$  fragments (see Fig. 1b) is always a Ni isotope. Due to the symmetry of the detector setup, namely to the fact that the two  $L_1, L_2$  fragments are always detected in coincidence with the same heavy fragments, one must also observe events with a missing Ni fragment. This is indeed observed, the peak corresponding to missing masses of 70 and 68 a.m.u. is well-seen in Fig. 4 (curve *b*). Thus the different peaks in the missing-mass spectrum consistently correspond all to the ternary decay scenario proposed.

Inspecting the lower part of Fig. 5a, we observe a gross bump, which is well bounded by the mass of the double magic nucleus of  ${}^{48}\text{Ca}$ . Further there is a strong manifestation for the formation of the deformed magic  ${}^{150}\text{Ce}$  nucleus [14], which is seen as two peaks (all in all 355 events) in the upper right corner of Fig. 5a ( ${}^{72,78}\text{Ni}/{}^{150}\text{Ce}$ ). Also a weak trace of a vertical ridge in the vicinity of the well-known magic  ${}^{144}\text{Ba}_{88}$  nucleus should be noted.

Completing this section, we would like to stress that the observation of structures for the masses of the emitted fragments and the missing masses corresponding to known shells must be seen as a decisive argument in favor of the physical origin of the effect of tripartition. No experimental feature can emphasize these mass values; the experiment does not know magic numbers. The role of the nuclear shells in the effect observed appears in analogy with known molecular-like states in light alpha-cluster nuclei, which can also form strongly deformed hyper-deformed resonances. Recent theoretical studies of multicluster accompanied fission [15] and binary clusterization of the  ${}^{252}\text{Cf}$  nucleus [16] emphasize the role of double magic nuclei of  ${}^{132}\text{Sn}$  and  ${}^{48}\text{Ca}$  in these processes.

## 5. CONCLUSION, THE TERNARY FISSION PROCESS

Understanding of the physical mechanism of the CCT will require additional efforts in experiment and theory, but some conclusions can already be drawn. The observed ternary decay must be viewed as a sequence of two neck ruptures of a hyperdeformed shape, and strongly deformed substructures may be created in the first step. In the ternary decay modes, first a heavy fragment may be created, equal by mass to the sum of two magic clusters (consisting of Sn, Te for the heavy and of Ge, Ni for the light ones) and a complementary light fragment  $L_1$ . The following rupture of the heavy fragment, created in the first stage, leads to the formation of cluster  $L_2$  and a complimentary one being heavier than Sn or Te. An alternative scenario leading to the horizontal ridge in Fig. 5a differs by the creation of Ni cluster at the first step.

We can consider a preformation of two magic clusters in the body of the fissioning system at the early stage of its elongation. This was shown in the framework of Strutinsky procedure in [17] to occur by the formation of a potential valley in a multidimensional deformation space. Descending from the fission barrier along a specific valley is accompanied by tunneling of the system into the valley of separated fragments [18]; this path is described by a continuous trajectory in the space of observables [19] relevant for the experiment such as energy, mass and others.

We can propose that the ternary decays follow the path along the most populated valley based on the Ge-Sn clusters revealed in ref. [17] and those energetically close by. All these valleys give rise to the trajectories which are united in the gross bump marked 7 in Figs. 2a and 5a.

Two important facts must be emphasized to explain the occurrence of the ternary fission in the specific mode observed here. Already from the liquid drop model the Q-value for the fission mode with three fragments is larger than for binary fission. Similar to the latter ternary fission is preferred for masses where magic numbers of the shell model are possible. The mentioned fission valleys are thus deeper than for binary fission and are deepest for ternary fission with at least two magic (or semimagic) clusters. The Coulomb interaction between the two clusters give the minimum energy value (deepest valley) for the collinear configuration. Deviations from these two conditions have very large effect in the reduction of the fission probabilities. The results presented here for the decay of the nucleus of the  $^{252}\text{Cf}$  show that the first time the true ternary spontaneous decay channel has been observed with good statistical accuracy in agreement with recent theoretical expectations [20]. The decay fragments with the masses in the vicinity of magic  $^{132}\text{Sn}$ ,  $^{70}\text{Ni}$  and  $^{48}\text{Ca}$  isotopes fly apart almost collinearly and we call such decay *collinear cluster tripartition (CCT)*. The probability of this new effect is not less than  $4 \cdot 10^{-3}$

with respect to the normal binary fission. This implies that its probability is much larger than that of the known ternary fission accompanied by the light charged particles. It seems now clear that the effect is due to the formation of the multicomponent nuclear molecules based on magic nuclei as clustered substructures in the body of the decaying heavy system. This observation points to the need of an essential refinement of the actual fission theory.

*Acknowledgements.* The work was partially supported by the Russian Foundation for Basic Research, grant 05-02-17493.

## REFERENCES

1. P. Schall *et al.*, On symmetric tripartition in the spontaneous fission of  $^{252}\text{Cf}$ , Phys. Let., **B 191**, 339 (1987).
2. S.P. Tretjakova *et al.*, The present state of cluster radioactivity research, Jadernaja fizika, **66**, 1665 (2003).
3. Yu.V. Pyatkov *et al.*, *Experimental confirmation of the collinear cluster tripartition of the  $^{252}\text{Cf}$  nucleus*, International Symposium on Exotic Nuclei, Peterhof, Russia, 5–12 July 2004, Conference proceedings, eds. Yu.E. Penionzhkevich, and E.A. Cherepanov, World Scientific, Singapore, p. 351–356, 2005.
4. Yu.V. Pyatkov *et al.*, *New indications of collinear tripartition in  $^{252}\text{Cf}(\text{sf})$  studied at the modified FOBOS setup*, Physics of Atomic Nuclei, **66**, 1631 (2003).
5. Yu.V. Pyatkov *et al.*, *New results in studying of the collinear cluster tripartition of the  $^{252}\text{Cf}$  nucleus*, JINR Preprint E15-2004-65, Dubna, 2004.
6. D.V. Kamanin *et al.*, *Neutron channel of the FOBOS spectrometer for the study of spontaneous fission*, Physics of Atomic Nuclei, **66**, 1655, (2003).
7. H.-G. Ortlepp *et al.*, *The  $4\pi$ -fragment-spectrometer FOBOS*, Nucl. Instr. and Meth. A, **403**, 65, (1998).
8. L. Meyer, *Plural and multiple scattering of low-energy heavy particles in solids*, Phys. Stat. Sol. (b), **44**, 253 (1971).
9. F. Goennenwein *et al.*, *Ternary and quaternary fission*, Europhysics news, **36**, 11 (2005).
10. M.A. Mariscotti, *A method for automatic identification of peaks in the presence of background and its application to spectrum analysis*, Nucl. Instr. and Meth, **50**, 309 (1967).
11. Yu.V. Pyatkov *et al.*, *Manifestation of the fine structures in the fission fragment mass-energy distribution in the  $^{233}\text{U}(n_{\text{th}}, f)$  reaction*, Nucl. Instr. and Meth., **A 488**, 381 (2002).
12. B.D. Wilkins *et al.*, *Scission-point model of nuclear fission based on deformed-shell effects*, Phys. Rev. C, **14**, 1832 (1976).
13. D. Rochman *et al.*, *Super-asymmetric fission in the  $^{245}\text{Cm}(n_{\text{th}}, f)$  reaction at the Lohengrin fission-fragment mass-separator*, Nucl. Phys., **A 735**, 3 (2004).
14. H. Márton, Private communication.
15. D.N. Poenaru *et al.*, *Multicluster accompanied fission*, Phys. Rev., **C 59**, 3457 (1999).
16. J. Cseh *et al.*, *Deformation dependence of nuclear clusterization*, Phys. Rev., **C 70**, 034311 (2004).
17. Yu.V. Pyatkov *et al.*, *Manifestation of clustering in the  $^{252}\text{Cf}(\text{sf})$  and  $^{249}\text{Cf}(n_{\text{th}}, f)$  reactions*, Nucl. Phys., **A 624**, 140 (1997).

- 
18. J.F. Berger *et al.*, *Microscopic analysis of collective dynamics in low energy fission*, Nucl. Phys., **A 428**, 23 (1984).
  19. Yu.V. Pyatkov *et al.*, *Nontrivial manifestation of clustering in fission of heavy nuclei at low and middle excitations*, Physics of Atomic Nuclei, **67**, 1726 (2004).
  20. D.N. Poenaru *et al.*, *Fission into Equally Sized Three Fragments*, Proc. Symposium on Nuclear Clusters, Rauschholzhausen, Germany, 5–9 August 2002, p. 283.